L-type Ca^{2+} current as the predominant pathway of Ca^{2+} entry during I_{Na} activation in β-stimulated cardiac myocytes

Franco DelPrincipe, Marcel Egger and Ernst Niggli

Department of Physiology, University of Bern, Bühlplatz 5, CH-3012 Bern, Switzerland

(Received 5 April 2000; accepted after revision 9 June 2000)

1. In the present study Ca^{2+} entry via different voltage-dependent membrane channels was examined with a fluorescent Ca^{2+} indicator before and after β-adrenergic stimulation.

2. To clearly distinguish between Ca^{2+} influx and Ca^{2+} release from the sarcoplasmic reticulum the Ca^{2+} store was blocked with 0·1 μM thapsigargin and 10 μM ryanodine. Omitting Na^+ from the pipette filling solution minimized Ca^{2+} entry via Na^+–Ca^{2+} exchange.

3. Individual guinea-pig ventricular myocytes were voltage clamped in the whole-cell configuration of the patch-clamp technique and different membrane currents were activated using specific voltage protocols. The intracellular Ca^{2+} concentration was simultaneously recorded with a laser-scanning confocal microscope using fluo-3 as a Ca^{2+} indicator.

4. Ca^{2+} entry pathways were discriminated using pharmacological blockers under control conditions and during β-adrenergic stimulation with 1 μM isoproterenol (isoprenaline) in the bathing solution or 100 μM cAMP in the patch-clamp pipette.

5. Isoproterenol or cAMP potentiated the Ca^{2+} influx signals recorded during L-type Ca^{2+} current activation but, more interestingly, also during Na^+ current (I_{Na}) activation. The Ca^{2+} influx signal arising from L-type Ca^{2+} current activation was usually blocked by 50 μM Cd^{2+}. However, the Ca^{2+} influx signal elicited by the Na^+ current activation protocol was only curtailed to 56·4 ± 28·2 % by 100 μM Ni^{2+} but was reduced to 17·9 ± 15·1 % by 50 μM Cd^{2+} and consistently eliminated by 5 mM Ni^{2+}.

6. The pronounced Cd^{2+} and moderate Ni^{2+} sensitivity of the Ca^{2+} influx signals suggested that the predominant source of Ca^{2+} influx during the Na^+ current activation – before and during β-adrenergic stimulation – was a spurious activation of the L-type Ca^{2+} current, presumably due to voltage escape during Na^+ current activation.

7. Calculations based on the relationship between Ca^{2+} current and fluorescence change revealed that, on average, we could reliably detect rapid Ca^{2+} concentration changes as small as 5·4 ± 0·7 nM. Thus, we can estimate an upper limit for the Ca^{2+} permeability of the phosphorylated TTX-sensitive Na^+ channels which is less than 0·04:1 for Ca^{2+} ions flowing through Na^+ channels via the proposed 'slip-mode' Ca^{2+} conductance. Therefore the slip-mode Ca^{2+} conductance of Na^+ channels does not contribute noticeably to the Ca^{2+} signals observed in our experiments.

Excitation–contraction coupling (EC coupling) and Ca^{2+} signalling in cardiac muscle are thought to be mediated by Ca^{2+} influx via the L-type Ca^{2+} current which subsequently triggers a much larger Ca^{2+} release from the sarcoplasmic reticulum (SR) by Ca^{2+}-induced Ca^{2+} release (CICR) (Fabiato, 1985; Bers, 1991). In contrast, skeletal muscle EC coupling is believed not to require an influx of Ca^{2+}. Instead, a direct mechanical connection links the voltage sensors with the SR Ca^{2+} release channels to control Ca^{2+} release by an allosteric interaction (Schneider & Chandler, 1973; Rios *et al.* 1992). Recently, several additional pathways that may trigger Ca^{2+} release from the SR of cardiac muscle have been proposed. These include Ca^{2+} entry via the voltage-sensitive Na^+–Ca^{2+} exchange during the depolarization (Levi *et al.* 1994), possibly enhanced by subsarcolemmal Na^+ accumulation during I_{Na} activation (Leblanc & Hume, 1990; Lipp & Niggli, 1994). In addition, Ca^{2+} influx via the T-type Ca^{2+} current has been reported to trigger slow CICR (Sipido *et al.* 1998).

Even more trigger pathways have been noted in cardiac muscle after β-adrenergic stimulation. One of these

mechanisms has been attributed to Ca^{2+} influx via TTX-sensitive Na^+ channels occurring after phosphorylation ('slip-mode Ca^{2+} conductance'; Santana *et al.* 1998; Cruz *et al.* 1999). By analogy with skeletal muscle, the existence of a purely voltage-activated SR Ca^{2+} release mechanism operating in the same voltage range has also been proposed (Hobai *et al.* 1997*b*; Ferrier *et al.* 1998). However, after β-adrenergic stimulation the CICR mechanism may operate under a high gain regime where a tiny influx of Ca^{2+} could be sufficient to trigger Ca^{2+} release. It is very difficult to rule out a small amount of Ca^{2+} entry via, for example, incompletely blocked Ca^{2+} channels (Trafford & Eisner, 1998). Therefore, we decided to apply a fluorescent indicator technique to examine Ca^{2+} influx via voltage-dependent membrane channels activated during the voltage-clamp protocols used in this study, both before and during β-stimulation. To analyse Ca^{2+} influx without contamination by Ca^{2+} release from the SR, CICR was suppressed with ryanodine and SR Ca^{2+} uptake was blocked with thapsigargin, except in a few initial control experiments. Ca^{2+} influx via the Na^+–Ca^{2+} exchange was minimized by omitting Na^+ from the pipette filling solution because this pathway has been investigated in separate studies (Lipp & Niggli, 1994; Niggli & Lipp, 1996). Preliminary findings on the analysed Ca^{2+} influx pathways have been communicated to the Biophysical Society in abstract form (DelPrincipe *et al.* 1999).

METHODS

Cell preparation

Experiments were performed on single ventricular myocytes isolated from the guinea-pig (*Cavia porcellus*). Adult animals were killed by cervical dislocation and the hearts rapidly removed and retrogradely perfused on a Langendorff perfusion system at 37 °C. The perfusion solution contained (mM): NaCl 135, KCl 5·4, $MgCl_2$ 1, NaH_2PO_4 0·33, Hepes 5, glucose 11, pH adjusted to 7·3 with NaOH. After 5 min, collagenase B (Boehringer Mannheim, Rotkreuz, Switzerland) and protease type XIV (Sigma, Buchs, Switzerland) were added to final concentrations of 0·2 mg ml^{-1} and 0·04 mg ml^{-1}, respectively, and the perfusion continued for another 4–6 min. Subsequently, the ventricles were minced and placed in perfusion solution containing 200 μM $CaCl_2$ on a rocking table to allow for dissociation of the tissue.

Cells were taken from the supernatant, transferred into a recording chamber with a coverslip floor and mounted onto the stage of an inverted microscope (Diaphot TMD, Nikon, Küsnacht, Switzerland). Ca^{2+} resistant cells readily adhered to the uncoated coverslip and were constantly superfused (1–2 ml min^{-1}) with extracellular solution containing (mM): NaCl 140, KCl 5, $MgCl_2$ 1, $CaCl_2$ 1, Hepes 10, glucose 10, pH adjusted to 7·4 with NaOH. Most experiments were carried out at room temperature (22 °C), but some control experiments were performed at 37 °C.

Electrophysiological recordings

Recording electrodes were pulled from filamented borosilicate glass capillaries (GC150F, Clark Electromedical Instruments, Pangbourne, UK) on a horizontal puller (DMZ, Zeitz Instrumente, Augsburg, Germany) and filled with intracellular solution containing (mM): caesium aspartate 120, TEA-Cl 20, Hepes 10, MgATP 5, $MgCl_2$ 1, fluo-3 0·1, pH adjusted to 7·2 with CsOH. Sodium was omitted to minimize Ca^{2+} entry via reverse-mode operation of the Na^+–Ca^{2+} exchanger. Typical pipette resistances were around 2 MΩ. Cells were voltage clamped in the whole-cell configuration and held at −70 mV without correction for junction potentials using an Axopatch 200 amplifier (Axon Instruments, Foster City, CA, USA).

Na^+ inward currents were activated by holding the voltage at −90 mV for 1·5 s before stepping to −40 mV for 50 ms. In the presence of 5 mM Ni^{2+} we observed a shift of the Na^+ current activation curve of about +20 mV which was due to surface charge screening effects (McLaughlin, 1989). Therefore, to activate a Na^+ current of similar amplitude in the presence of 5 mM Ni^{2+} the voltage was stepped to −20 mV. L-type Ca^{2+} currents were activated by holding the voltage at −40 mV for 1·5 s before stepping to +10 mV for 200 ms. During the Ca^{2+} release experiments, the cells were paced with a series of depolarizing voltage pulses (from −70 to 0 mV for 200 ms at 1 Hz) before each sweep to activate L-type Ca^{2+} currents and refill the SR.

Series resistance was compensated to about 60–75% with the built-in compensation circuit of the amplifier. Current recordings showing poor voltage control due to changes in series resistance were not used for analysis. No on-line leak subtraction was performed. For calculations, where the pure Ca^{2+} current was to be integrated, the current recorded in the presence of 50 μM Cd^{2+} was subtracted off-line. Currents were low-pass filtered at 5 or 10 kHz and digitized at 10 kHz using an A/D converter and the LabView acquisition software (National Instruments, Ennetbaden, Switzerland). Data were stored on hard disk for later analysis with the IgorPro software (WaveMetrics, Lake Oswego, OR, USA).

Confocal Ca^{2+} measurements

Cells were viewed with a ×63 oil-immersion objective lens (Neofluar, NA = 1·25, Zeiss, Oberkochen, Germany) and loaded with fluo-3 through the recording pipette. Fluo-3 was excited with the 488 nm line of an argon laser (model 5000, Ion Laser Technology, Salt Lake City, USA) at 150 μW intensity on the cell. The fluorescence was detected at 540 ± 15 nm with the photomultiplier tube (PMT) of a laser-scanning confocal system (MRC 1000, Bio-Rad, Glattbrugg, Switzerland) operated in the line-scan mode. The scan speed was set to 2 or 6 ms per line. The 512 lines recorded in one frame thus corresponded to 1·024 or 3·072 s, respectively. When long current trains were recorded, the speed was set to 13·28 ms per line. Each line-scan image contained a signal from a red light diode which was synchronized with the voltage protocol and recorded with the second PMT of the confocal system (> 600 nm).

Fluorescence images were processed using a customized version of the public domain NIH Image program (developed at the US National Institutes of Health and available on the Internet at http://rsb.info.nih.gov/nih-image/). Mean Ca^{2+} concentration profiles were extracted from fluorescence images and calculated with the IgorPro software using an established self-ratio calibration procedure (Cheng *et al.* 1993). We assumed a resting Ca^{2+} concentration of 100 nM at the beginning of each experiment and a K_d for fluo-3 of 500 nM.

Materials

All chemicals used were of reagent grade and dissolved in distilled water of cell culture grade. Thapsigargin and tetrodotoxin (TTX) were purchased from Alomone Labs (Jerusalem, Israel), ryanodine from Calbiochem (La Jolla, CA, USA), isoproterenol ([−]-*N*-isopropyl-L-noradrenaline hydrochloride) from Fluka (Buchs,

Switzerland), cAMP (adenosine 3′,5′-monophosphate, free acid) from Sigma (Buchs, Switzerland) and fluo-3 (pentapotassium salt) from TefLabs (Austin, TX, USA).

Cells were incubated with thapsigargin and ryanodine for 30 min after the dissociation process to block the SR Ca^{2+} pump and the ryanodine receptor. Thapsigargin was dissolved as 1 mM stock in ethanol and used at 0·1 μM. Ryanodine was dissolved as 1 mM stock in distilled water and used at a concentration of 10 μM. Isoproterenol was freshly prepared as a 10 mM stock in an aqueous 1 mM L-ascorbic acid solution before each experiment and added at a concentration of 1 μM to the extracellular solution. Cyclic AMP was freshly prepared as a 10 mM aqueous stock and added to the pipette solution at a concentration of 100 μM. Drugs were delivered to the cells by means of a gravity-driven rapid superfusion system placed in the vicinity (~200 μm) of the cell selected for an experiment.

RESULTS

Potentiation of Ca^{2+} signals by β-adrenergic stimulation

In most experiments we used isoproterenol as an agonist for the β-adrenergic receptors. The β-adrenergic receptors represent the starting point of the signalling cascade leading to elevated levels of cAMP and subsequent activation of protein kinases (for reviews, see Tsien, 1977; Reuter, 1983). The main advantage of isoproterenol over cAMP is its convenient and rapid extracellular administration, which allowed us to record data under control and test conditions in one and the same cell. In addition, by comparing test data with control values we could check for the presence of the complete signalling cascade. The concentration of isoproterenol used, 1 μM, is about 100-fold the EC_{50} (Katsube *et al.* 1996; Calaghan *et al.* 1998) and was chosen to activate a large fraction of the β-receptors. To assess the effects of isoproterenol on the Ca^{2+} current, the Na^+ current and Ca^{2+} release from the SR, we applied a specific voltage protocol based on the activation and inactivation curves of each current. L-type Ca^{2+} currents were activated by depolarizing from a holding potential of −40 mV to +10 mV for 200 ms, whereas Na^+ currents were activated by depolarizing the cell from −90 mV to −40 mV for 50 ms (Weidmann, 1955). In previous experiments we had confirmed that under our experimental conditions we activated maximal currents and that the currents were separable with these voltage protocols. This could be verified from the amplitudes and from the distinct time courses of the two currents.

Figure 1 shows representative results obtained from two cells. In the absence of ryanodine and thapsigargin activation of L-type Ca^{2+} currents produced large Ca^{2+} signals as a result of Ca^{2+} influx and CICR from the SR (Fig. 1*A*, left panel). The administration of 1 μM isoproterenol to the same cell resulted in a ~2-fold potentiation of both the L-type Ca^{2+} current and the Ca^{2+} transient (Fig. 1*A*, right panel). In most cells, activation of the Na^+ current produced a clear Ca^{2+} signal which was markedly smaller than that produced by activation of the

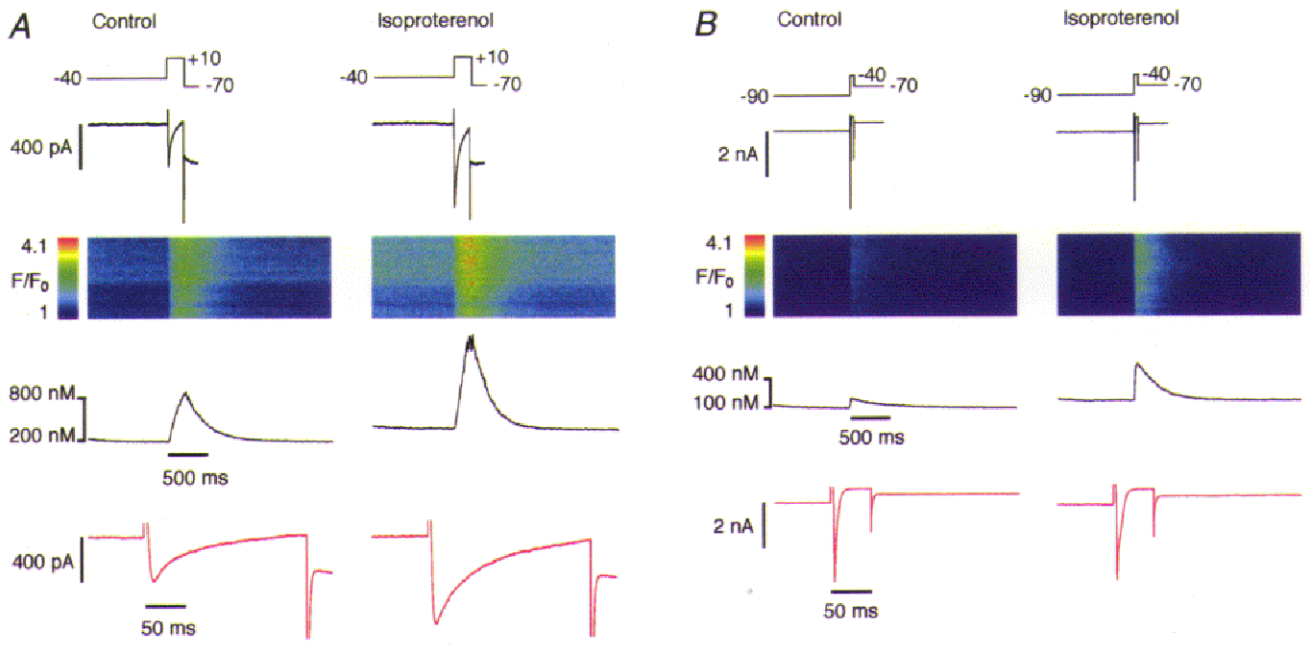

Figure 1. Simultaneous recording of inward current and Ca^{2+} release

A, activation of the L-type Ca^{2+} current (200 ms) elicited a substantial Ca^{2+} release signal. Both the current and the Ca^{2+} signal were markedly enhanced by administration of 1 μM isoproterenol in the bathing solution. *B*, in an analogous experiment, activation of the Na^+ current (50 ms) in a different cell showed smaller Ca^{2+} signal amplitudes but similar β-adrenergic potentiation. Traces show from top to bottom: voltage protocol (mV), current record, line-scan image, mean Ca^{2+} concentration profile, same current record expanded 10 times (red traces, not temporally aligned to the other signals).

Ca^{2+} current, even before β-adrenergic stimulation (Fig. 1*B*, left panel; note change in scale). In some cells, no Ca^{2+} signal could be detected at all during a Na^+ current voltage-clamp protocol. However, after the application of 1 μM isoproterenol the Ca^{2+} signal either increased in amplitude (Fig. 1*B*, right) or became visible in the cells where it was not detectable in the control solution. The Ca^{2+} signals activated by I_{Na} had a faster onset than the Ca^{2+} signals activated by I_{Ca}, typically peaking within 6 ms. Occasionally, the inactivation of I_{Na} appeared to be slowed down and formed a shoulder in the inactivation phase of the current (Fig. 1, expanded current traces shown in red; see below for discussion). In general, the amplitude of the recorded I_{Na} was quite variable among different cells under both control conditions and β-adrenergic stimulation.

Potentiation of Ca^{2+} influx by β-adrenergic stimulation

As mentioned above, the positive feedback of CICR can vary considerably under different SR Ca^{2+} loads (Han *et al.* 1994; Spencer & Berlin, 1995; Bassani *et al.* 1995). The gain can reach levels where the influx of a minute amount of Ca^{2+} could trigger some Ca^{2+} release from the SR by Ca^{2+}-induced Ca^{2+} release, which then becomes self-sustaining. Particularly in the presence of high levels of cAMP, the SR Ca^{2+} pump is disinhibited due to phosphorylation of phospholamban, whereby Ca^{2+} uptake into the SR is increased and Ca^{2+} release is enhanced (Tsien & Weingart, 1976; Calaghan *et al.* 1998). An increased SR Ca^{2+} load presumably renders the SR Ca^{2+} release channels more sensitive to trigger Ca^{2+} (Györke & Györke, 1998). To obtain direct information about the various Ca^{2+} influx pathways and how they might be modulated by β-adrenergic stimulation we used pharmacological tools that allowed us to reduce the complexity inherent in cardiac Ca^{2+} signalling. For this purpose, we suppressed the SR Ca^{2+} release and uptake with 10 μM ryanodine and 0·1 μM thapsigargin. Thus, after the initial control experiments shown above, we recorded Ca^{2+} signals arising exclusively from Ca^{2+} influx via the plasmalemma and we relied on the confocal microscope system for the detection of Ca^{2+} influx signals without any amplification by the SR. Residual SR activity would manifest itself in the form of Ca^{2+} sparks or Ca^{2+} waves in the line-scan images. Figure 2 shows examples of Ca^{2+} influx signals elicited by I_{Ca} and I_{Na} in a cell with blocked SR function. The amplitudes of the Ca^{2+} influx transients were severalfold smaller than in cells not treated with ryanodine and thapsigargin, confirming the absence of a Ca^{2+} release component (note the absence of sparks). Nevertheless, a potentiation of the Ca^{2+} influx transient by isoproterenol was still evident in all cells analysed with both voltage-clamp protocols (i.e. during both I_{Ca} and I_{Na}).

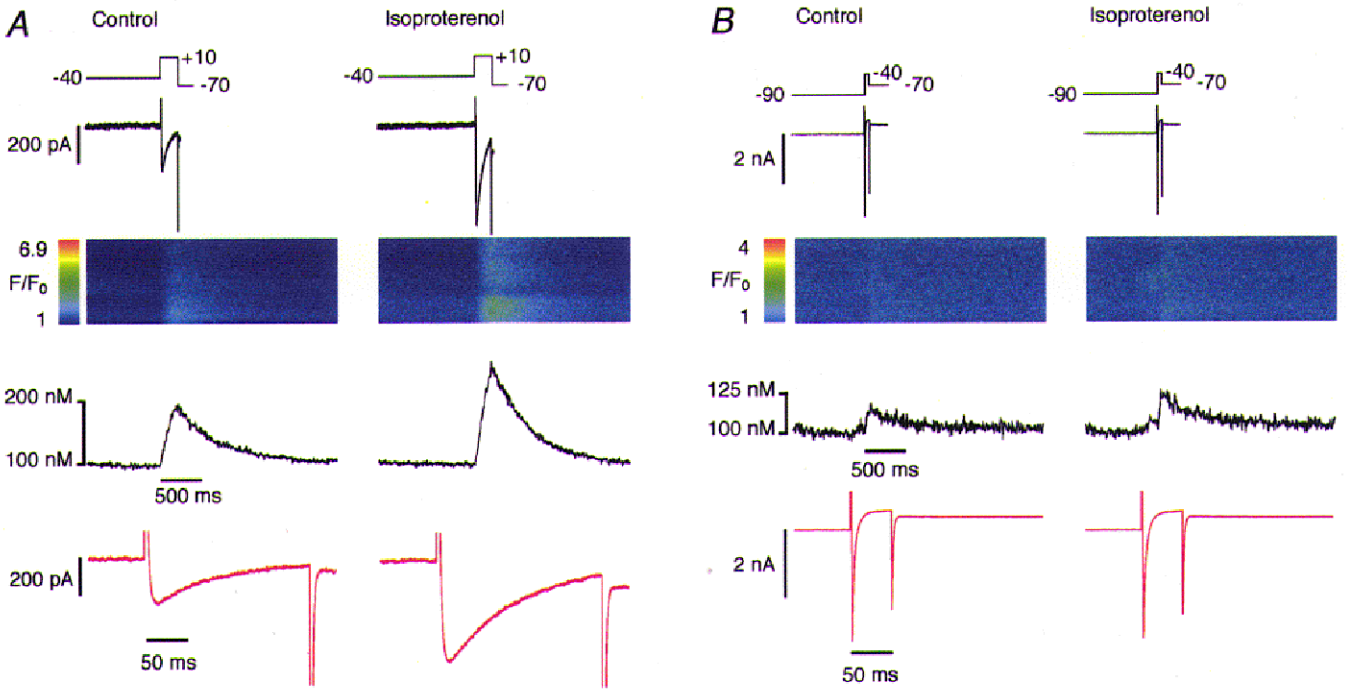

Figure 2. Simultaneous recording of inward current and Ca^{2+} influx

SR Ca^{2+} release was blocked by treating the cells with 0·1 μM thapsigargin and 10 μM ryanodine. Na^+ current was activated in the presence of 1 μM isoproterenol. *A*, activation of L-type Ca^{2+} current elicited an detectable Ca^{2+} influx signal with reduced amplitude due to the blockade of the SR release (note the absence of sparks). A potentiating effect of isoproterenol on the current amplitude and the Ca^{2+} signal is evident. *B*, analogous experiment with activation of the Na^+ current. Note the change in the scale and the small amplitude of the Ca^{2+} signals. Traces are arranged in the same way as in Fig. 1.

Identification of Ca^{2+} influx pathways during β-adrenergic stimulation

While an increase of the Ca^{2+} influx signal via L-type Ca^{2+} current during β-adrenergic stimulation can easily be explained by the known effect of L-type Ca^{2+} channel phosphorylation (Kameyama *et al.* 1985; Katsube *et al.* 1996), the reason for the changes observed during the I_{Na} activation protocol was not clear. Having a reproducible experimental protocol available to show the significant potentiating effect of β-stimulation on Ca^{2+} influx, we tried

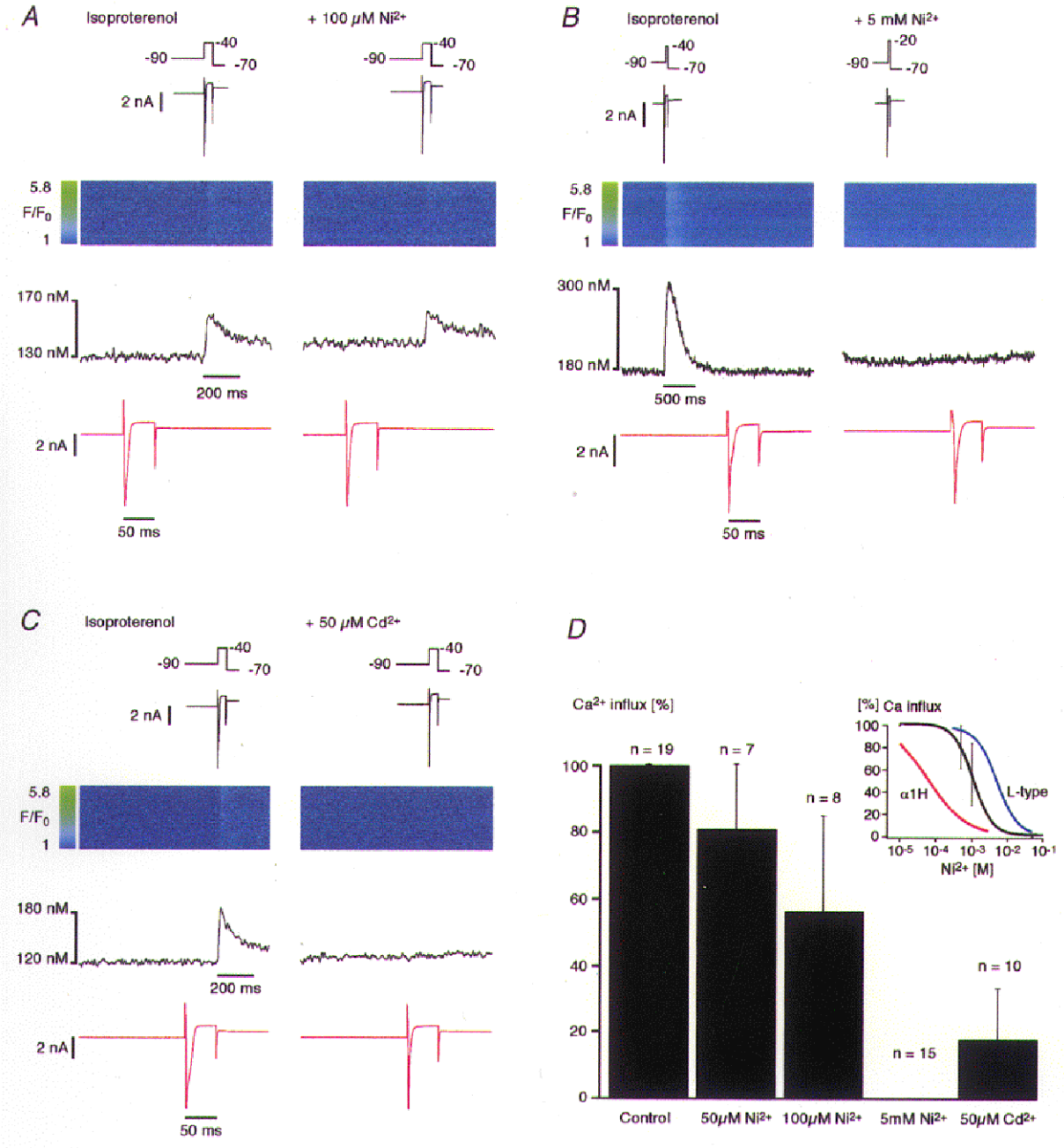

Figure 3. Pharmacological identification of the Ca^{2+} influx pathway

All cells were treated with 0·1 μM thapsigargin and 10 μM ryanodine. Na^+ current was activated in the presence of 1 μM isoproterenol. *A*, the administration of 100 μM Ni^{2+} failed to block the Ca^{2+} influx signal. However, a slight reduction of the Ca^{2+} signal amplitude is noticeable. *B*, the administration of 5 mM Ni^{2+} blocked the Ca^{2+} signal completely. *C*, the Ca^{2+} influx signal was eliminated by 50 μM Cd^{2+}. Traces are arranged in the same way as in Fig. 1. *D*, normalized Ca^{2+} influx amplitudes *versus* different concentrations of Ni^{2+} and of 50 μM Cd^{2+}. Data are plotted as means ± S.D. The inset shows a Hill function fitted to the data points of the Ni^{2+} block. The calculated IC_{50} was 114 ± 33·2 μM (95% confidence); the Hill coefficient was 1·71. For comparison, the Hill function of the Ni^{2+} dose–response curves of the L-type current in guinea-pig ventricular myocytes (blue trace, taken from Hobai *et al.* 1998) and in the human heart T-type α1H subunit (T-type, red trace, taken from Lee *et al.* 1999) have been added.

to identify the Ca^{2+} entry pathway that, first, was enhanced by β-stimulation and, second, was manifest during the voltage-clamp protocol designed to activate I_{Na} only. Considering the known Ca^{2+} entry pathways present in heart cells (Bers, 1991; Boyett *et al.* 1996), we used pharmacological tools to block L- and T-type Ca^{2+} channels and also the Na^+–Ca^{2+} exchanger.

Initially, we applied various concentrations of Ni^{2+}, an ion that is known to block T-type Ca^{2+} currents at micromolar concentrations and L-type Ca^{2+} currents (and the Na^+–Ca^{2+} exchange current, $I_{Na\text{-}Ca}$) at millimolar concentrations (McDonald *et al.* 1994; Lee *et al.* 1999). The effect of Ni^{2+} on the Ca^{2+} influx signal observed during I_{Na} in our experiments was strongly dose dependent (see Fig. 3). The Ca^{2+} influx amplitude was reduced to $80{\cdot}9 \pm 19{\cdot}4\%$ of the control by 50 μM Ni^{2+} ($n = 7$). With 100 μM Ni^{2+} in the extracellular solution the Ca^{2+} influx signal amplitude was $56{\cdot}4 \pm 28{\cdot}2\%$ of the control ($n = 8$). Interestingly, the Ca^{2+} influx signal elicited by I_{Na} activation was only reduced to undetectable levels by a high concentration of Ni^{2+} (5 mM; $n = 15$ cells). Figure 3*B* shows the blocking effect of 5 mM Ni^{2+} on a substantial Ca^{2+} influx signal. Note that in the presence of 5 mM Ni^{2+} the activation curve for I_{Na} was shifted by +20 mV and thus we had to depolarize the cell to −20 mV to elicit a comparable current amplitude (Fig. 3*B*, right panel, top trace). Thus, it appeared that millimolar concentrations of Ni^{2+} were required to reliably suppress Ca^{2+} influx during the voltage-clamp protocol designed to elicit I_{Na}.

For a quantitative analysis the averaged and normalized Ca^{2+} influx amplitudes were plotted against the Ni^{2+} concentration and fitted with a Hill function (Fig. 3*D*, inset). The function revealed an IC_{50} of $114 \pm 33{\cdot}2$ μM (confidence interval 95%) and a Hill coefficient of about 1·71. These values are approximately in the same range as the values obtained for Ni^{2+}-induced block of the L-type Ca^{2+} current in guinea-pig ventricular myocytes stimulated with 100 μM cAMP (IC_{50} of about 510 μM and a Hill coefficient of about 1·48: Hobai *et al.* 1998; see Fig. 3*D*, inset, blue line). For comparison, the Hill function of the human heart T-type α-subunit (α1H) is also plotted in the same graph (Fig. 3*D*, inset, red line). The dose–response data for this line were obtained from recombinant α1H subunits expressed in human embryonic kidney HEK-293 cells or *Xenopus* oocytes (Lee *et al.* 1999). In contrast to the L-type Ca^{2+} current, these data yielded an IC_{50} of about 12 μM (HEK-293) or 5·7 μM (oocytes), with Hill coefficients of about 0·77. It is worth noting that we measured fluorescence changes caused by Ca^{2+} influx and not a membrane current. Thus, a direct comparison is not straightforward. Nevertheless, the IC_{50} for Ni^{2+}-induced block of Ca^{2+} influx that we obtained is comparable to that for L-type Ca^{2+} channels but 10- to 20-fold higher than that for the T-type Ca^{2+} channels.

The next tool we used was Cd^{2+} which should noticeably block the L-type Ca^{2+} current at 50 μM while minimally affecting the T-type Ca^{2+} current or the Na^+–Ca^{2+} exchanger (Hobai *et al.* 1997*a*). Figure 3*C* shows the blocking effect of

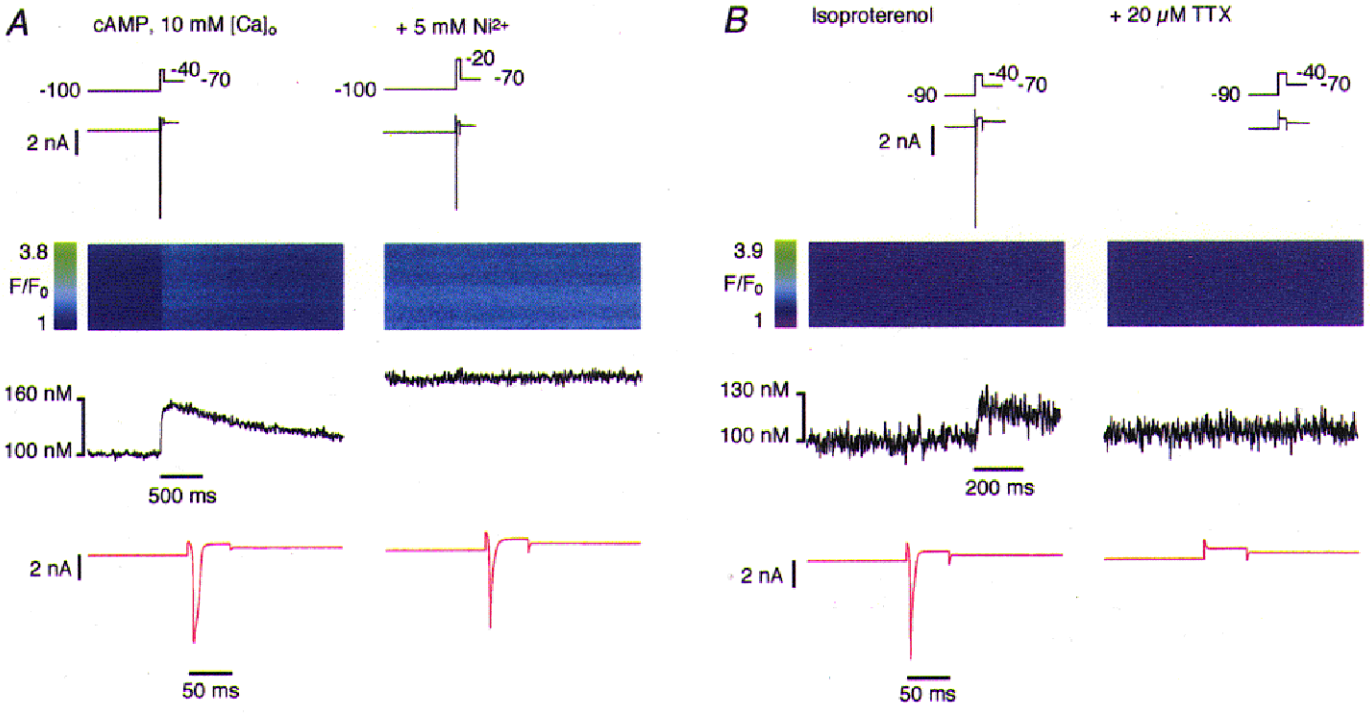

Figure 4. Ca^{2+} influx under elevated cAMP and blockade by TTX

A, with 100 μM cAMP in the pipette filling solution, activation of I_{Na} elicited a Ca^{2+} influx signal which was blocked by 5 mM Ni^{2+}. Note the increase in fluorescence in the right line-scan, which is due to elevated extracellular Ca^{2+} (10 mM). *B*, the Na^+ current and the Ca^{2+} influx signal elicited in the presence of 1 μM isoproterenol were completely blocked by 20 μM TTX.

50 μM Cd^{2+} on the Ca^{2+} influx signal. This low dose of Cd^{2+} reduced the Ca^{2+} influx signal observed during I_{Na} activation to an average of 17·9 ± 15·1 % of control values ($n = 10$; Fig. 3*D*). In addition, the shoulder present during I_{Na} inactivation was removed by this inhibitor, suggesting that it was carried by a Cd^{2+}-sensitive current, most likely the L-type Ca^{2+} current. The clear-cut effect of Cd^{2+}, suggesting Ca^{2+} influx via L-type Ca^{2+} channels, does not imply that other sources of Ca^{2+} cannot contribute to a Ca^{2+} signal under different conditions, particularly when Na^+–Ca^{2+} exchange is not minimized (Leblanc & Hume, 1990; Lipp & Niggli, 1994; Niggli & Lipp, 1996) or when the amplification by SR Ca^{2+} release is not suppressed (Santana *et al.* 1998).

We were also interested in examining whether the same results could be reproduced by elevating intracellular cAMP directly via the patch pipette instead of applying isoproterenol. In these experiments the concentration of cAMP in the pipette solution was 100 μM to provide maximal stimulation of cAMP-dependent protein kinase (Kameyama *et al.* 1985). In addition, the high concentration in the pipette was necessary to counteract the reduction in cAMP concentration caused by phosphodiesterase activity (Kameyama *et al.* 1985). To maximize putative Ca^{2+} entry via phosphorylated sodium channels (Santana *et al.* 1998), we also increased extracellular Ca^{2+} to 10 mM in some of these experiments. The results obtained in the presence of intracellular cAMP were essentially the same as those with isoproterenol added to the bath. Figure 4*A* shows a representative recording where the Ca^{2+} influx signal, in the presence of 100 μM cAMP in the pipette, was completely abolished by 5 mM Ni^{2+}.

To provide evidence that the Ca^{2+} influx signal we observed was related to I_{Na} and not to the voltage change or to shifts of I_{Ca} activation and gating we blocked the Na^+ channels with 10–20 μM TTX. Figure 4*B* shows that as I_{Na} disappeared after application of 20 μM TTX the Ca^{2+} influx signal also vanished, suggesting that activation of I_{Na} is indeed required to initiate the observed Ca^{2+} influx.

Ca^{2+} influx during trains of I_{Na}

Inspired by a recent report on Ca^{2+} influx via sodium channels (Santana *et al.* 1998), we adopted a strategy designed to favour Ca^{2+} entry through this proposed pathway using a vigorous voltage-clamp protocol. To obtain better control over the voltage we used lower resistance electrodes (~1 MΩ) and attempted to elicit larger Na^+ currents. In addition, we applied trains of I_{Na} in order to accumulate the presumably small Ca^{2+} influx signal which we otherwise might have missed with our detection system (see below).

Figure 5*A* documents an experiment where we applied a train of 50 depolarizing voltage pulses at 33 Hz in the presence of 1 μM isoproterenol. Care was taken to space the

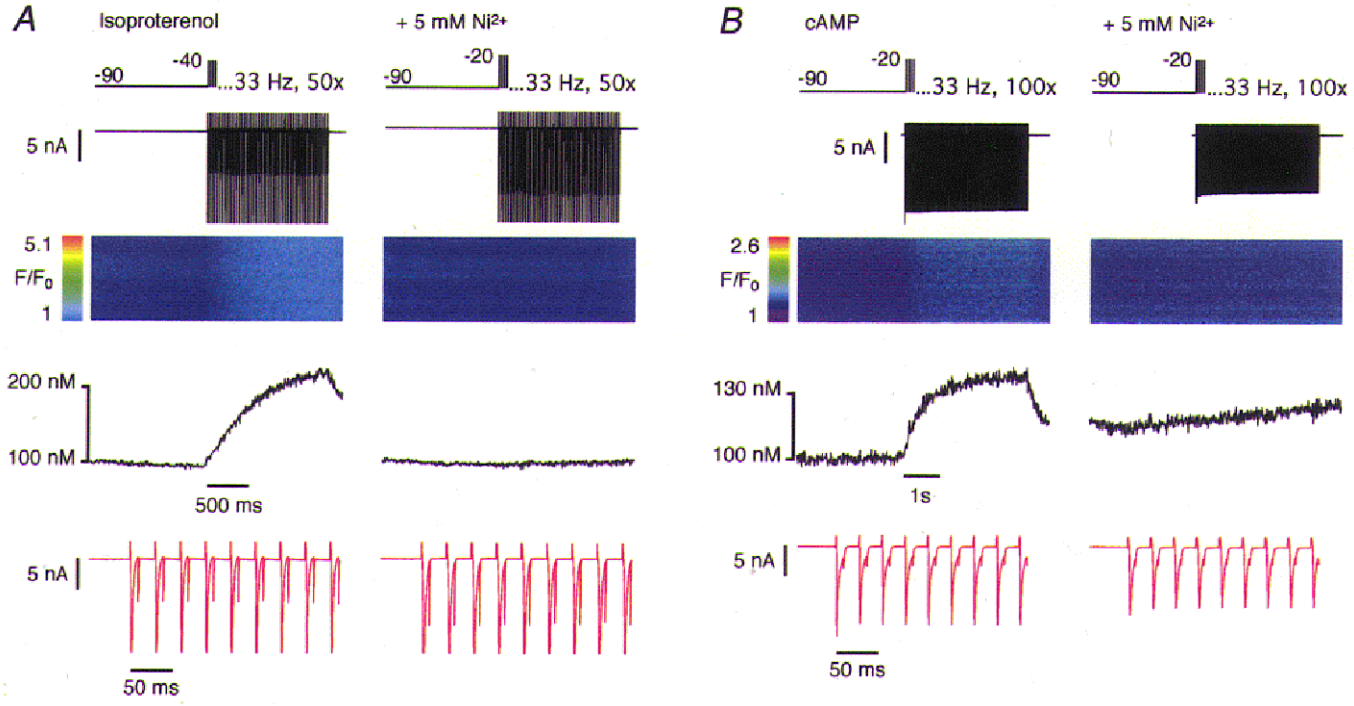

Figure 5. Forced Ca^{2+} influx under extreme conditions

SR release was blocked and the Na^+ current was activated repetitively in the presence of 1 μM isoproterenol. *A*, a Ca^{2+} influx signal could be elicited by a train of 50 depolarizing pulses at 33 Hz. The Ca^{2+} influx signal was eliminated by 5 mM Ni^{2+}. *B*, an analogous experiment was performed in the absence of isoproterenol but with 100 μM cAMP in the pipette filling solution. Sodium currents were activated repetitively 100 times at 33 Hz.

pulses appropriately to allow I_{Na} to recover from inactivation. This protocol led to a substantial current amplitude (Fig. 5*A*, expanded current shown in red). The Ca^{2+} influx signal increased progressively during the train reaching a plateau at the end (Fig. 5*A*, left). However, the Ca^{2+} influx signal was again completely abolished in the presence of 5 mM Ni^{2+} (Fig. 5*A*, right). Figure 5*B* shows a similar experiment that was performed with 100 μM cAMP in the pipette instead of administration of isoproterenol and with a train of 100 depolarizing pulses. Once more, the Ca^{2+} influx was abolished by 5 mM Ni^{2+}. To test whether the proposed Ca^{2+} influx through TTX-sensitive Na^+ channels was sensitive to temperature under these conditions, like, for instance, the proposed voltage-sensitive Ca^{2+} release (Hobai *et al.* 1997*b*; Ferrier *et al.* 1998), the same experiments were repeated at 37 °C ($n = 6$). The results were identical to those observed at room temperature (data not shown).

Sometimes a small and slowly progressive elevation of the resting Ca^{2+} concentration was detectable (see, for example, Figs 3*B* and 5*B*). However, this rise did not coincide temporally with the voltage-clamp pulses. This monotonic rise in $[Ca^{2+}]_i$ may be attributed to block of the Na^+–Ca^{2+} exchanger by 5 mM Ni^{2+} which prevented any extrusion of Ca^{2+} entering by slow leakage through the plasmalemma.

Estimation of the detection limit for Ca^{2+} entry

As we relied on confocal Ca^{2+} fluorescence measurements to detect Ca^{2+} influx across the sarcolemma, we were interested in determining the detection limit of our system. This would enable us, based on theoretical assumptions, to estimate the minimal amount of Ca^{2+} entering the cell that can be detected. In addition, we could indirectly calculate the maximal permeability of TTX-sensitive Na^+ channels to Ca^{2+} ions that would be consistent with our results. Since we were dealing with changes in Ca^{2+} concentration, the

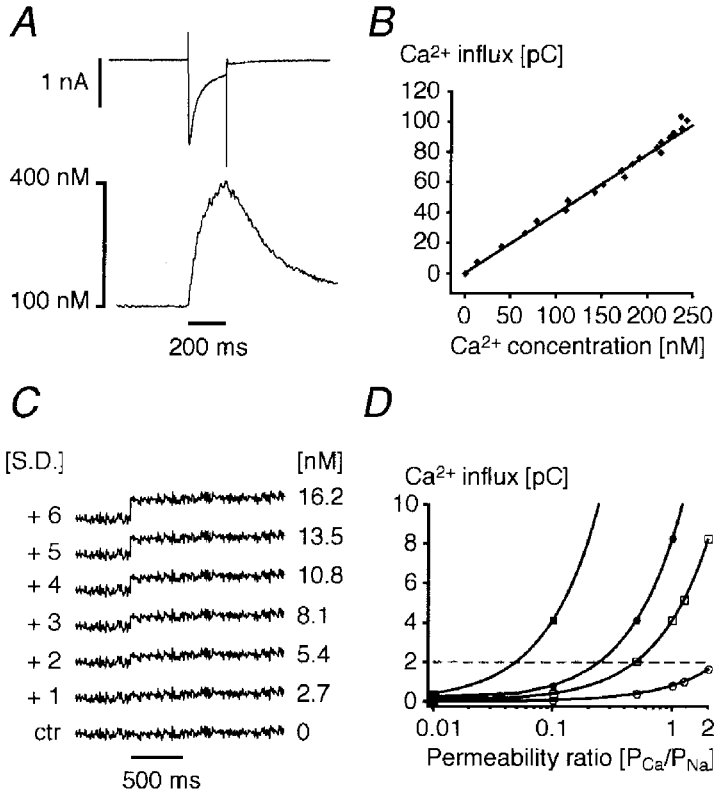

Figure 6. Estimation of the detection limit and relationship to a calculated permeability ratio

A, in a cell with blocked SR CICR an L-type Ca^{2+} current and the resulting Ca^{2+} influx signal were recorded simultaneously under control conditions. *B*, the Cd^{2+}-sensitive difference current was integrated and plotted against the rising phase of the Ca^{2+} signal. The fitted line relates the observed Ca^{2+} influx fluorescence amplitude to the corresponding Ca^{2+} current in this given cell and corresponds to a cytosolic buffer capacity of about 28 (note that the SR was blocked). *C*, an mean Ca^{2+} concentration profile was plotted from a line-scan image and the standard deviation of the noise was calculated. After 500 ms, a step increase in Ca^{2+} was simulated by adding a concentration jump corresponding to a multiple of the S.D. The first step that is clearly visible coincides with +3 S.D. and, for this particular cell, corresponds to a concentration change of ~8 nM $[Ca^{2+}]_i$. Taking the relationship illustrated in *B* we can estimate our mean detection limit for Ca^{2+} influx to be around 2 pC (dashed horizontal line in *D*). *D*, using the Goldmann-Hodgkin-Katz equation, the permeability ratio P_{Ca}/P_{Na} was calculated for a 50 nA (□, ■) or 10 nA Na^+ current (○, ●) and for 10 mM (●, ■) or 1 mM $[Ca^{2+}]_o$ (○, □), respectively.

relevant parameter determining the detection limit was the signal-to-noise ratio of the fluorescence record. Therefore, we determined the noise in a typical line-scan image recorded at the beginning of an experiment. We assumed a resting Ca^{2+} concentration of 100 nM and a K_d of fluo-3 for Ca^{2+} of 500 nM, values on which we based our calibrations for all data presented. Statistical analysis of different mean Ca^{2+} concentration profiles yielded a mean noise level of $1{\cdot}78 \pm 0{\cdot}24$ nM (r.m.s. ± S.D., $n = 10$).

In a subsequent computer simulation, we added step increases of $[Ca^{2+}]$ to a Ca^{2+} concentration profile recorded from one particular cell and were thus mimicking the Ca^{2+} influx signal observed during I_{Na} activation (Fig. 6). The amplitudes of the steps corresponded to multiples of the standard deviation of the noise derived from the same record. We identified the $[Ca^{2+}]$ step which we could detect by eye and defined our detection limit to be 3 standard deviations of the noise. This turned out to be ~8 nM in the fairly noisy record shown in Fig. 6, or ~5·34 nM on average. It is well known that each calibration procedure relies on several assumptions. The K_d of fluo-3 in the cytoplasmic environment can differ considerably from the *in vitro* value (Harkins *et al.* 1993). In addition, in the presence of a low intracellular Na^+ concentration the resting Ca^{2+} concentration could be lower than 100 nM in a quiescent guinea-pig myocyte, because a low $[Na^+]_i$ increases the driving force of the Na^+–Ca^{2+} exchanger for Ca^{2+} removal. However, calibrating with a K_d of 1000 nM instead of 500 nM would not change the Ca^{2+} concentrations appreciably (they would increase by factor of ~1·2) whereas assuming a resting $[Ca^{2+}]$ of 50 nM would improve our detection limit by a factor of ~2·4 (data not shown).

Finally, we could relate the observed Ca^{2+} concentration change to Ca^{2+} influx using the relationship between the measured and numerically integrated Ca^{2+} current (Cd^{2+}-sensitive difference) and the corresponding Ca^{2+} influx fluorescence signal (Fig. 6*A*). The linear relationship obtained by plotting the integral of the Ca^{2+} current *versus* the Ca^{2+} concentration allowed us to determine the minimal Ca^{2+} influx needed to produce a detectable Ca^{2+} signal, which on average was ~2 pC (Fig. 6*B*). Based on this amount of charge it is possible to calculate the maximal permeability of the Na^+ channel to Ca^{2+} which would be consistent with our data. The Goldmann-Hodgkin-Katz current equation (Hille, 1992) of the form:

$$I_S = P_S z_S^2 EF^2/RT \times \{([S]_i - [S]_o \exp(-z_S EF/RT))/(1 - \exp(-z_S EF/RT))\},$$

was used to calculate the absolute permeability for Na^+ at the ionic concentrations, membrane potential and measured current obtained under our experimental conditions. We introduced the ionic concentrations for Na^+ ($[S]_i = 1$ mM, $[S]_o = 140$ mM), the charge ($z_S = +1$), and the driving force ($E = E_m - E_S = -164$ mV for these Na^+ concentrations) and calculated the absolute permeability P_S for assumed current amplitudes. F stands for the Faraday constant, R for the universal gas constant and T for the absolute temperature. The index 'S' refers to the ionic species in question. By introducing assumed values for the absolute permeability of Ca^{2+} (P_S) into the same equation and taking the variables $[S]_i$, $[S]_o$, z_S and E for Ca^{2+} we derived a fractional current amplitude (I_S) carried by Ca^{2+} ions.

This current was numerically integrated to obtain a theoretical Ca^{2+} influx. The Ca^{2+} permeability was expressed as permeability ratio, P_{Ca}/P_{Na}, and plotted against the expected Ca^{2+} influx (Fig. 6*D*). The horizontal dashed line separates the detectable Ca^{2+} influx signals (above) from the undetectable signals (below). It represents the mean detection limit calculated from the mean noise (1·78 nM) using a K_d of 500 nM and a resting $[Ca^{2+}]$ of 100 nM. Whole-cell patch-clamp Na^+ current measurements usually underestimate the real current amplitude because of the access resistance. For large Na^+ currents (50 nA: Brown *et al.* 1981; Makielski *et al.* 1987) and high extracellular Ca^{2+} (10 mM) we should detect signals elicited by single Na^+ currents corresponding to a permeability ratio of about 0·04:1. Furthermore, the detection for Ca^{2+} influx during trains consisting of 50 or 100 Na^+ currents would be considerably more sensitive. Using the same noise analysis procedure we estimated that we could detect a slow elevation of Ca^{2+} concentration during a current train if the deviation from a control trace at the end of the train corresponded to ~8 nM (or 3 S.D. of the noise). Therefore, the detection limit in a train would correspond to about 0·16 nM per single Na^+ current or to a Ca^{2+}/Na^+ permeability ratio of 0·0012 : 1.

DISCUSSION

The Ca^{2+} influx signals mainly result from activation of L-type Ca^{2+} channels

During voltage-clamp protocols designed to activate L-type Ca^{2+} currents our experimental results confirmed the expected changes in Ca^{2+} influx after β-adrenergic stimulation. Activation of β-receptors is known to induce a signalling cascade which ultimately leads to phosphorylation of various Ca^{2+} signalling proteins and membrane channels by protein kinase A (PKA), including the L-type Ca^{2+} channels (Kameyama *et al.* 1985). After PKA phosphorylation, L-type Ca^{2+} channels exhibit a higher open probability (Tsien *et al.* 1986). In contrast, the mechanism underlying the increase in the Ca^{2+} influx signals during voltage-clamp protocols tailored to specifically activate Na^+ currents was less clear. Before reaching a conclusion, several experimental difficulties and possible pitfalls need to be considered. It is well known that Na^+ currents have very large amplitudes in cardiac myocytes (Brown *et al.* 1981; Makielski *et al.* 1987). Consequently, it is notoriously difficult, if not impossible, to control the clamp voltage during the activation of the current with conventional amplifiers and patch-clamp recording pipettes (Makielski *et al.* 1987; Hüser *et al.* 1996). As a consequence, during I_{Na} activation the

membrane potential briefly escapes away from the imposed clamp potential towards the Na^+ reversal potential and hence towards the voltage range for the activation of L-type Ca^{2+} currents. In principle, L-type Ca^{2+} channels could be activated and carry Ca^{2+} influx during such voltage escape. Since the L-type Ca^{2+} channels are phosphorylated by cAMP-dependent protein kinase after β-stimulation, the Ca^{2+} influx signal generated during voltage escape may become larger after the application of isoproterenol. In addition, it has to be considered that isoproterenol not only increases the amplitude of I_{Ca} but also shifts its activation threshold towards more negative potentials (Katsube *et al.* 1996). This may lead to the activation of some L-type Ca^{2+} channels during the I_{Na} protocol (at −40 mV) after β-stimulation. The proposed voltage-activated Ca^{2+} release mechanism has also been reported to be facilitated by β-stimulation (Hobai *et al.* 1997*b*; Ferrier *et al.* 1998). However, in the present study any Ca^{2+} release from the SR was eliminated by ryanodine and thapsigargin and a contribution by SR Ca^{2+} release can thus be excluded. Other Ca^{2+} entry pathways which may possibly be involved are discussed below.

Considering all these pitfalls and after analysing the voltage sensitivity and the pharmacological profile of the Ca^{2+} influx signal observed in this study, we reached the conclusion that the major fraction of these Ca^{2+} influx signals was indeed generated by spurious activation of L-type Ca^{2+} channels during escape of the membrane potential from voltage clamp. β-Stimulation of these channels then led to a more pronounced manifestation of this effect, presumably by increasing the open probability and by shifting the activation of the L-type Ca^{2+} channels. Several lines of evidence suggested this conclusion. First, the analysis of the current traces (I_{Na}) revealed an apparent slowing of inactivation after exposure to isoproterenol. In some cases a distinct shoulder appeared during the late phase of the inactivation, indicating that another current had been activated (Fig. 3*C*). Interestingly, this shoulder, as well as the Ca^{2+} influx signal, turned out to be Cd^{2+} sensitive. Second, the sensitivity of the Ca^{2+} influx signal to 5 mM Ni^{2+} also suggested the participation of either the L- or T-type Ca^{2+} current (or both). However, the small or absent effect of low concentrations of Ni^{2+} (50–100 μM) indicates that T-type Ca^{2+} channels contribute very little, if at all, since they are known to exhibit a much higher Ni^{2+} sensitivity (Sipido *et al.* 1998; but see also Lee *et al.* 1999). In this case, the relatively small effect of low Ni^{2+} concentrations on the influx of Ca^{2+} could be explained by the known overlap of the dose–response curves for T- and L-type Ca^{2+} channels (i.e. even low Ni^{2+} concentrations have a minor blocking effect on L-type Ca^{2+} current). The almost complete block by 50 μM Cd^{2+}, which is an indicator of the involvement of the L-type Ca^{2+} current (Hobai *et al.* 1997*a*), provides strong support for the view that most of the Ca^{2+} influx during the I_{Na} protocol was carried by L-type Ca^{2+} channels. As mentioned above, the depolarisation to −40 mV during the I_{Na} activation protocol could activate a small fraction of the L-type Ca^{2+} channels, particularly following the leftward shift in activation after β-stimulation. However, the disappearance of the Ca^{2+} influx signal upon administration of 20 μM TTX clearly suggests that the depolarization to −40 mV did not *per se* induce any detectable Ca^{2+} influx, not even after β-stimulation. This result can be explained if block of I_{Na} with TTX prevents voltage escape. The following experimental observation provides further support for this view. When the series resistance compensation of the voltage-clamp amplifier was impaired on purpose, the Ca^{2+} influx signals during I_{Na} activation clearly increased in amplitude (not shown). Thus, precise control of the membrane potential seems to prevent the activation of I_{Ca}.

Involvement of T-type Ca^{2+} channels

We expected that the I_{Na} activation protocol (depolarization from −90 mV to −40 mV) would also activate T-type Ca^{2+} currents which could have led to a noticeable Ca^{2+} influx. However, the weak sensitivity of the Ca^{2+} signal to 50 μM Ni^{2+}, a concentration which was shown to be discriminative for cardiac T-type Ca^{2+} channels (Sipido *et al.* 1998; Lee *et al.* 1999), suggests that this pathway only contributed a small fraction of the detectable Ca^{2+} influx. It is also worth mentioning that the T-type Ca^{2+} current has been reported to be insensitive to β-stimulation in the guinea-pig heart (Tytgat *et al.* 1988; Balke *et al.* 1993; but see Vassort & Alvarez, 1994). Based on these findings and on the Cd^{2+} sensitivity discussed above, we believe that a significant participation of the T-type Ca^{2+} channels in the generation of a Ca^{2+} influx signal sensitive to β-stimulation is unlikely.

Contribution of the Na^+–Ca^{2+} exchanger to the Ca^{2+} influx signal

In the present study, we were concerned with Ca^{2+} influx via voltage-dependent membrane channels and therefore tried to minimize the reverse mode Na^+–Ca^{2+} exchange by omitting Na^+ from the intracellular solution. It is clear, however, that this procedure cannot completely prevent some accumulation of Na^+ close to the membrane during I_{Na} activation, which in turn could elicit a small Ca^{2+} influx via Na^+–Ca^{2+} exchange (Lederer *et al.* 1990; Lipp & Niggli, 1994; Niggli & Lipp, 1996). In our experiments, this pathway would also be blocked by 5 mM Ni^{2+}. Therefore this pathway is indistinguishable from spurious activation of I_{Ca} based on this observation alone. However, it has to be pointed out that the Ca^{2+} influx signal observed in the absence of Na^+ in the pipette filling solution was suppressed by the administration of 50 μM Cd^{2+} or the L-type Ca^{2+} channel blocker nifedipine (10 μM; not shown). Cd^{2+} is known to block the Na^+–Ca^{2+} exchange only at much higher concentrations (IC_{50} 320 μM; Hobai *et al.* 1997*a*). Taken together, these findings strongly suggest that Ca^{2+} influx via the Na^+–Ca^{2+} exchanger only played a small role when Na^+ was omitted from the patch pipette solution.

Other sources for Ca^{2+} influx

Potential additional pathways for Ca^{2+} influx via Na^+ channels have been reported recently in guinea-pig (Cole *et*

al. 1997) and rat ventricular myocytes (Aggarwal *et al.* 1997). These voltage-activated currents were blocked by TTX and were insensitive to 50 μM Ni^{2+}. However, no evidence was provided that Ca^{2+} influx really occurred, nor that Ca^{2+} release could be triggered. Moreover, the current presumably carried by Ca^{2+} ions in these experiments was only observed when Na^+ was completely absent from the extracellular solution because Na^+_o blocked the current at micromolar concentrations. Since we used physiological Na^+ concentrations in all experiments, the participation of these currents in generating a Ca^{2+} influx can be excluded.

The possibility of Ca^{2+} permeation through TTX-sensitive Na^+ channels, even with physiological extracellular Na^+ concentrations, was discussed several years ago (Sorbera & Morad, 1990; Johnson & Lemieux, 1991; Hume *et al.* 1991; Lederer *et al.* 1990). Recently, experimental support for this controversial pathway has been reported by Santana *et al.* (1998). They observed SR Ca^{2+} release triggered by Ca^{2+} apparently entering through TTX-sensitive Na^+ channels, but only after β-adrenergic stimulation. In addition, the permeability ratio P_{Ca}/P_{Na} was shifted from almost 0 : 1 to 1·25 : 1. This newly described peculiarity of the Na^+ channels was termed 'slip-mode Ca^{2+} conductance'. A salient feature of this proposed mode of conductance is the insensitivity of the Ca^{2+} release to 5 mM Ni^{2+}.

Since this TTX-sensitive β-stimulation-dependent Ca^{2+} influx signal had several characteristics resembling the Ca^{2+} influx signals observed in the present study, we also tried to detect Ca^{2+} influx via slip-mode conductance, taking advantage of the insensitivity of the influx to 5 mM Ni^{2+}. This allowed us to supress all other known Ca^{2+} entry pathways with a single unspecific blocker. During such experiments, we anticipated that the Ca^{2+} fluorescence signal would be small since we had suppressed any amplification by CICR. The estimate of the detection limit of our confocal fluorescence measurement suggested that we should be able to detect Ca^{2+} influx through slip-mode conductance during a single I_{Na} as soon as the Ca^{2+}/Na^+ permeability ratio exceeded 0·04 : 1. This estimate of the detection limit is very conservative because the real Na^+ current is presumably larger than the measured current. Indeed, experiments carried out with low access resistance electrode systems had suggested peak currents of up to 140 nA in rat ventricular myocytes (Brown *et al.* 1981; Makielski *et al.* 1987). For trains of 100 I_{Na} activations, which rapidly accumulate the Ca^{2+} influx, the detection would be correspondingly more sensitive.

In conclusion, we believe that when Ca^{2+} entry via Na^+–Ca^{2+} exchange is minimized, and in the absence of blockers for L-type Ca^{2+} channels, escape of the voltage clamp, leading to spurious activation of L-type Ca^{2+} channels, is the most important pathway for Ca^{2+} influx during I_{Na} activation protocols. Ca^{2+} entry via the slip-mode conductance of the Na^+ channels did not participate in the generation of measureable Ca^{2+} influx under our experimental conditions. In principle, a much smaller Ca^{2+} influx than ~8 nM into the diadic space could still be sufficient to trigger Ca^{2+} release from the SR, but such a small slip-mode conductance would then not be consistent with the Ca^{2+}/Na^+ permeability ratio determined from shifts of the reversal potential (Santana *et al.* 1998).

Aggarwal, R., Shorofsky, S. R., Goldman, L. & Balke, C. W. (1997). Tetrodotoxin-blockable calcium currents in rat ventricular myocytes; a third type of cardiac cell sodium current. *Journal of Physiology* **505**, 353–369.

Balke, C. W., Rose, W. C., O'Rourke, B., Mejia-Alvarez, R., Backx, P. & Marban, E. (1993). Biophysics and physiology of cardiac calcium channels. *Circulation* **87**, VII-49–VII-53.

Bassani, J. W. M., Yuan, W. L. & Bers, D. M. (1995). Fractional SR Ca release is regulated by trigger Ca and SR Ca content in cardiac myocytes. *American Journal of Physiology* **37**, C1313–1319.

Bers, D. M. (1991). *Excitation-Contraction Coupling and Cardiac Contractile force.* Kluwer Academic, Dortrecht, Boston, London.

Boyett, M. R., Harrison, S. M., Janvier, N. C., McMorn, S. O., Owen, J. M. & Shui, Z. (1996). A list of vertebrate cardiac ionic currents: nomenclature, properties, function and cloned equivalents. *Cardiovascular Research* **32**, 455–481.

Brown, A. M., Lee, K. S. & Powell, T. (1981). Sodium current in single rat heart muscle cells. *Journal of Physiology* **318**, 479–500.

Calaghan, S. C., White, E. & Colyer, J. (1998). Co-ordinated changes in cAMP, phosphorylated phospholamban, Ca^{2+} and contraction following β-adrenergic stimulation of rat heart. *Pflügers Archiv* **436**, 948–956.

Cheng, H., Lederer, W. J. & Cannell, M. B. (1993). Calcium sparks: elementary events underlying excitation-contraction coupling in heart muscle. *Science* **262**, 740–744.

Cole, C. C., Chartier, D., Martin, M. & Leblanc, N. (1997). Ca^{2+} permeation through Na^+ channels in guinea pig ventricular myocytes. *American Journal of Physiology* **273**, H128–137.

Cruz, J. dos S., Santana, L. F., Frederick, C. A., Isom, L. L., Malhorta, J. D., Mattei, L. N., Kass, R. S., An, R. H. & Lederer, W. J. (1999). Whether 'slip mode conductance' occurs? (Technical comment). *Science* **284**, 711a.

DelPrincipe, F., Egger, M. & Niggli, E. (1999). Pathways for Ca^{2+} entry in cardiac myocytes. *Biophysical Journal* **76**, A462 (abstract).

Fabiato, A. (1985). Time and calcium dependence of activation and inactivation of calcium-induced release of calcium from the sarcoplasmic reticulum of a skinned canine cardiac Purkinje cell. *Journal of General Physiology* **85**, 247–289.

Ferrier, G. R., Zhu, J., Redondo, I. M. & Howlett, S. E. (1998). Role of cAMP-dependent protein kinase A in activation of a voltage-sensitive release mechanism for cardiac contraction in guinea-pig myocytes. *Journal of Physiology* **513**, 185–201.

Györke, I. & Györke, S. (1998). Regulation of the cardiac ryanodine receptor channel by luminal Ca^{2+} involves luminal Ca^{2+} sensing sites. *Biophysical Journal* **75**, 2801–2810.

Han, S., Schiefer, A. & Isenberg, G. (1994). Ca^{2+} load of guinea-pig ventricular myocytes determines efficacy of brief Ca^{2+} currents as trigger for Ca^{2+} release. *Journal of Physiology* **480**, 411–421.

Harkins, A. B., Kurebayashi, N. & Baylor, S. M. (1993). Resting myoplasmic free calcium in frog skeletal muscle fibers estimated with fluo-3. *Biophysical Journal* **65**, 865–881.

Hille, B. (1992). *Ionic Channels of Excitable Membranes*, 2nd edn. Sinauer Associates, Sunderland, MA, USA.

Hobai, I. A., Bates J. A., Howarth, F. C. & Levi, A. J. (1997*a*). Inhibition by external Cd^{2+} of Na/Ca exchange and L-type Ca^{2+} channel in rabbit ventricular myocytes. *American Journal of Physiology* **272**, H2164–2172.

Hobai, I. A., Hancox, J. C. & Levi, A. J. (1998). Inhibition of the L-type Ca^{2+} channel by external nickel in guinea-pig ventricular myocytes dialysed with cAMP-free and cAMP-containing solutions. *Journal of Physiology* **511.P**, 80*P* (abstract).

Hobai, I. A., Howarth, F. C., Pabbathi, V. K., Dalton, G. R., Hancox, J. C., Zhu, J. Q., Howlett, S. E., Ferrier, G. R. & Levi, A. J. (1997*b*). 'Voltage-activated Ca release' in rabbit, rat and guinea-pig cardiac myocytes, and modulation by internal cAMP. *Pflügers Archiv* **435**, 164–173.

Hume, J. R., Levesque, P. C. & Leblanc, N. (1991). Sodium-calcium exchange. *Science* **251**, 1370–1371.

Hüser, J., Lipp, P. & Niggli, E. (1996). Confocal microscopic detection of potential-sensitive dyes used to reveal loss of voltage control during patch-clamp experiments. *Pflügers Archiv* **433**, 194–199.

Johnson, E. A. & Lemieux, R. D. (1991). Sodium-calcium exchange. *Science* **251**, 1370–1371.

Kameyama, M., Hofmann, F. & Trautwein, W. (1985). On the mechanism of beta-adrenergic regulation of the Ca^{2+} channel in the guinea-pig heart. *Pflügers Archiv* **405**, 285–293.

Katsube, Y., Yokoshuki, H., Nguyen, L. & Sperelakis, N. (1996). Differences in isoproterenol stimulation of Ca^{2+} current of rat ventricular myocytes in neonatal compared to adult. *European Journal of Pharmacology* **317**, 391–400.

Leblanc, N. & Hume, J. R. (1990). Sodium current-induced release of calcium from cardiac sarcoplasmic reticulum. *Science* **248**, 372–376.

Lederer, W. J., Niggli, E. & Hadley, R. W. (1990). Sodium-calcium exchange in excitable cells: fuzzy space. *Science* **248**, 283.

Lee, J.-H., Gomora, J. C., Cribbs, L. L. & Perez-Reyes, E. (1999). Nickel block of three cloned T-type calcium channels: low concentrations selectively block α1H. *Biophysical Journal* **77**, 3034–3042.

Levi, A. J., Spitzer, K. W., Kohmoto, O. & Bridge, J. H. (1994). Depolarization-induced Ca^{2+} entry via Na^{+}-Ca^{2+} exchange triggers SR release in guinea pig cardiac myocytes. *American Journal of Physiology* **266**, H1422–1433.

Lipp, P. & Niggli, E. (1994). Sodium current-induced calcium signals in isolated guinea-pig ventricular myocytes. *Journal of Physiology* **474**, 439–446.

McDonald, T. F., Pelzer, S., Trautwein, W. & Pelzer, D. J. (1994). Regulation and modulation of calcium channels in cardiac, skeletal and smooth muscle cells. *Physiological Reviews* **74**, 365–507.

McLaughlin, S. (1989). The electrostatic properties of membranes. *Annual Review of Biophysics and Biophysical Chemistry* **18**, 113–137.

Makielski, J. C., Sheets, M. F., Hanck, D. A., January, C. T. & Fozzard, H. A. (1987). Sodium current in voltage clamped internally perfused canine cardiac Purkinje cells. *Biophysical Journal* **52**, 1–11.

Niggli E. & Lipp P. (1996). Elementary events of I_{Na}- and I_{Ca}-triggered EC coupling. *Biophysical Journal* **70**, A275 (abstract).

Reuter, H. (1983) Calcium channel modulation by neurotransmitters, enzymes and drugs. *Nature* **301**, 569–574.

Rios, E., Pizarro, G. & Stefani, E. (1992). Charge movement and the nature of signal transduction in skeletal muscle excitation-contraction coupling. *Annual Review of Physiology* **54**, 109–133.

Santana, L. F., Gomez, A. M. & Lederer, W. J. (1998). Ca^{2+} flux through promiscuous cardiac Na^{+} channels: slip-mode conductance. *Science* **279**, 1027–1033.

Schneider, M. F. & Chandler, W. K. (1973). Voltage dependent charge movement of skeletal muscle: a possible step in excitation-contraction coupling. *Nature* **242**, 244–246.

Sipido, K. R., Carmeliet, E. & Van de Werf, F. (1998). T-type Ca^{2+} current as a trigger for Ca^{2+} release from the sarcoplasmic reticulum in guinea-pig ventricular myocytes. *Journal of Physiology* **508**, 439–451.

Sorbera, L. A. & Morad, M. (1990). Atrionatiuretic peptide transforms cardiac sodium channels into calcium-conducting channels. *Science* **247**, 969–973.

Spencer, C. I. & Berlin, J. R. (1995). Control of sarcoplasmic reticulum calcium release during calcium loading in isolated rat ventricular myocytes. *Journal of Physiology* **488**, 267–279.

Trafford, A. W. & Eisner, D. A. (1998). Another trigger for the heartbeat. *Journal of Physiology* **513**, 1.

Tsien, R. W. (1977). Cyclic AMP and contractile activity in the heart. *Advances in Cyclic Nucleotide Research* **8**, 363–420.

Tsien, R. W., Bean, B. P., Hess, P., Lansman, J. B., Nilius, B. & Nowycky, M. C. (1986). Mechanisms of calcium channel modulation by beta-adrenergic agents and dihydropyridine calcium agonists. *Journal of Molecular and Cellular Cardiology* **18**, 691–710.

Tsien, R. W. & Weingart, R. (1976). Inotropic effect of cyclic AMP in calf ventricular muscle studied by a cut end method. *Journal of Physiology* **260**, 117–147.

Tytgat, J., Nilius, B., Vereecke, J. & Carmeliet, E. (1988). The T-type Ca channel in guinea-pig ventricular myocytes is insensitive to isoprotenerol. *Pflügers Archiv* **411**, 704–706.

Vassort, G. & Alvarez, J. (1994). Cardiac T-type calcium current: Pharmacology and roles in cardiac tissue. *Journal of Cardiovascular Pharmacology* **5**, 376–393.

Weidmann, S. (1955). The effect of the cardiac membrane potential on the rapid availability of the sodium carrying system. *Journal of Physiology* **127**, 213–224.

Acknowledgements

This work was supported by the Swiss National Science Foundation (grant no. 31-50564·97 to EN). We thank Dr S. Thomas for comments and correction of the manuscript and D. Lüthi for technical assistance.

Corresponding author

E. Niggli: Department of Physiology, University of Bern, Bühlplatz 5, CH-3012 Bern, Switzerland.

Email: niggli@pyl.unibe.ch

URL: http://beam.to/calcium_quark